AIP | Applied Physics Letters

# Nanometer-scale electrical characterization of stressed ultrathin SiO 2 films using conducting atomic force microscopy

M. Porti, M. Nafra, X. Aymerich, A. Olbrich, and B. Ebersberger

Citation: Applied Physics Letters **78**, 4181 (2001); doi: 10.1063/1.1382624
View online: http://dx.doi.org/10.1063/1.1382624
View Table of Contents: http://scitation.aip.org/content/aip/journal/apl/78/26?ver=pdfcov
Published by the AIP Publishing

# Nanometer-scale electrical characterization of stressed ultrathin $SiO_2$ films using conducting atomic force microscopy

M. Porti,[a] M. Nafría, and X. Aymerich
*Departament d' Enginyeria Electrònica, Universitat Autònoma de Barcelona, Edifici Cn, 08193 Bellaterra, Spain*

A. Olbrich and B. Ebersberger
*Infineon Technologies AG, Otto-Hahn Ring 6, 81730 Munich, Germany*

(Received 1 February 2001; accepted for publication 9 May 2001)

A conductive atomic force microscope has been used to electrically stress and to investigate the effects of degradation in the conduction properties of ultrathin (<6 nm) $SiO_2$ films on a nanometer scale (areas of $\approx$100 $nm^2$). Before oxide breakdown, switching between two states of well-defined conductivity and sudden changes of conductivity were observed, which are attributed to the capture/release of single charges in the defects generated during stress. © *2001 American Institute of Physics.* [DOI: 10.1063/1.1382624]

Although a great effort has been devoted to identifying the mechanisms that lead to the dielectric breakdown of thin $SiO_2$ films in metal–oxide–semiconductor (MOS) structures, the microscopic related phenomena are not completely understood yet. Nowadays, however, it is accepted that oxide failure is the consequence of progressive degradation of its structure (which has been related to the generation of defects) and that breakdown takes place in a very localized area ($10^{-12}$–$10^{-13}$ $cm^2$).[1] Present knowledge of the phenomena has been mostly gained from electrical stress on MOS capacitors of $\sim 10^{-3}$–$10^{-6}$ $cm^2$ areas (namely, from macroscopic tests), which provide spatially averaged information on oxide electrical properties. However, due to the extremely local nature of the phenomena, to completely understand the degradation and breakdown mechanisms, an investigation at a nanometer scale range is required. For this, scanning probe microscopy based techniques can be an alternative. Scanning tunneling microscopy (STM),[2,3] ballistic electron microscopy (BEEM),[4–6] and conducting atomic force microscopy (C-AFM)[7–10] have already been used to electrically characterize $SiO_2$ films with a resolution of a few nanometers. Among the different scanning probe microscopies, AFM techniques are more appropriate for the study of insulating surfaces and, from the experimental point of view, quite a bit simpler. Moreover, when an AFM is provided with a conductive tip (C-AFM), topographical and electrical information about the oxide can be simultaneously collected with a typical lateral resolution of ~10 nm. Despite this capability, and although the idea has been already suggested,[9] the use of C-AFM to study the physics of the degradation and breakdown processes has not yet been reported. In this letter, stress tests are applied to ultrathin $SiO_2$ films using a C-AFM (microscopic tests) and the electrical properties of the nanometric stressed $SiO_2$ areas are analyzed.

The electrical measurements were performed with an AFM from Digital Instruments (contact mode, working in air) equipped with a conductive tip (B-doped diamond) and a picoamp amplifier.[8] Electrons were injected from the substrate in order to avoid anodic oxidation processes[7,11] and the detrimental effects of any surface contamination.[7] Constant-voltage scans (while recording the current) and voltage ramps on a fixed oxide position (to measure the $I-V$ characteristics) can be performed. The top electrode of MOS structures (2.9, 4.2, and 5.9 nm ellipsometrical thick oxides thermally grown on an $n$-doped Si substrate) was removed to electrically characterize the bare oxides with the C-AFM. In this setup, the conductive tip is effectively the metal electrode of a MOS structure with a typical area of $\approx$100 $nm^2$.

Maps of current were obtained by applying scans at a constant voltage between the tip and the substrate. Figure 1(a) shows the current image measured on a fresh 5.9 nm thick oxide with a tip polarization of 6.4 V. The oxide shows nonhomogeneous electrical properties: some sites (spots) are brighter (larger current) than others, showing larger conductivity. The leaky sites have been considered to be the precursors of breakdown.[12] A statistical analysis of the image shows that the area of the spots is relatively constant and close to the estimated breakdown spot area (~100 $nm^2$).[1] Therefore, the C-AFM lateral resolution is large enough to resolve single oxide spots. Detailed electrical information on these spots has been obtained by measuring local $I-V$ data on a fixed oxide location. Figure 1(b) shows a typical $I-V$ characteristic (squares) measured with the C-AFM on a fresh oxide spot. The dashed lines correspond to the bounds in current measured over an area. Note that current densities through the oxide up to 10 $A/cm^2$ are allowed, and are comparable to those used during macroscopic high-field stress, so that degradation (and even breakdown) can be induced during these tests. The $I-V$ curves measured show Fowler–Nordheim (FN) behavior,[13] as expected for a MOS test structure. The FN current density [Eq. (1)] depends on two main oxide parameters: the injection barrier height ($\phi$) and the physical oxide thickness ($t_{ox}$).

[a]Electronic mail: marc.porti@uab.es



 

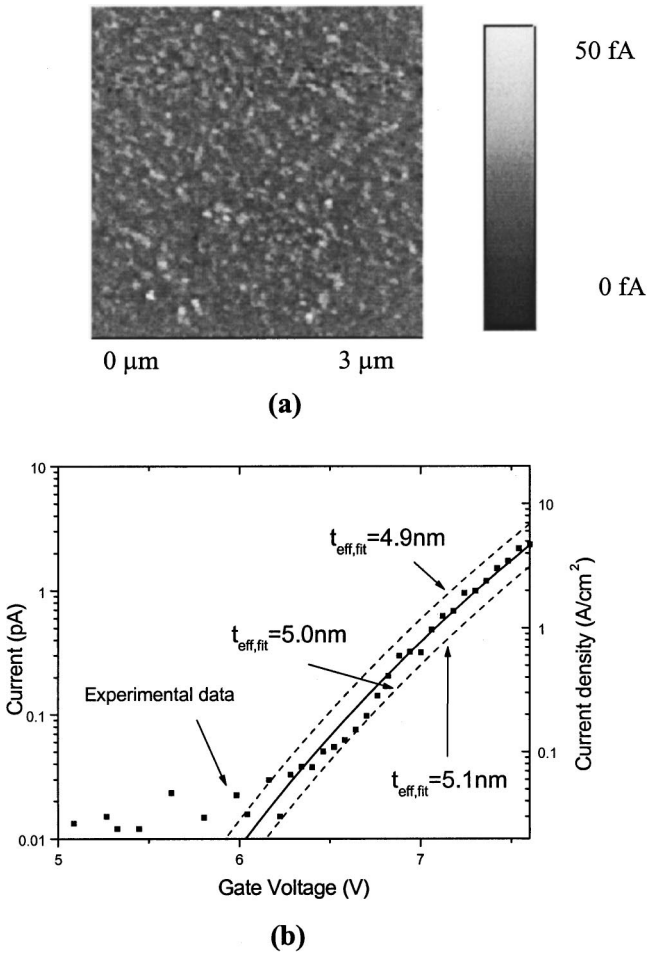


FIG. 1. (a) Image of current taken at 6.4 V on a fresh oxide area. The area of the observed spots has been estimated to be of the order of the breakdown spot area. (b) Experimental $I-V$ curve (squares) taken on a virgin spot, which has been fitted by the FN law (continuous line) with the electrical thickness as the unique parameter. The dashed lines correspond to the bounds in current observed over an area. Variations in $t_{\mathrm{eff}}$ as small as 0.1 nm can be measured.

$$J \propto \frac{V_{\mathrm{ox}}^2}{\Phi t_{\mathrm{ox}}^2} \exp\left(-C\frac{t_{\mathrm{ox}}}{V_{\mathrm{ox}}}\Phi^{3/2}\right) \overset{\phi=3.15\ \mathrm{eV}}{\Rightarrow} J \propto \frac{V_{\mathrm{ox}}^2}{t_{\mathrm{eff}}^2} \times \exp\left(-C'\frac{t_{\mathrm{eff}}}{V_{\mathrm{ox}}}\right), \quad (1)$$

with $C$ being a constant. By fixing the value of $\phi$ to 3.15 eV (the nominal value for the $Si-SiO_2$ interface), only one fitting parameter is needed, the electrical or effective thickness, $t_{\mathrm{eff}}$.[8] This parameter includes the dependence of the current on the physical thickness ($t_{\mathrm{ox}}$) and on the injection barrier height ($\phi$), as Eq. (1) shows ($C'$ is a constant). When measuring on a fixed oxide location (i.e., $t_{\mathrm{ox}}$ remains constant); any change in the oxide that affects the barrier height will be recorded as a change in the electrical thickness. In particular, the degradation induced during high-field stress (which is assumed to be related to the generation of defects) can modify the barrier height and, hence, $t_{\mathrm{eff}}$. For example, the trapping of an electron in a generated defect will increase $\phi$, leading to a lower current through the oxide, or, in other words, to a larger electrical thickness. Therefore, the effective thickness can be used as a monitor of the degradation.

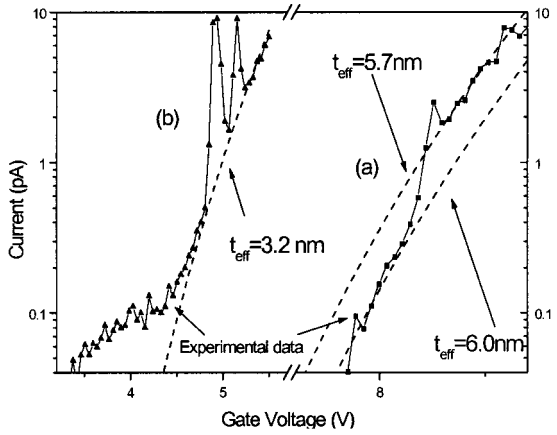


| Voltage | $t_{\mathrm{cathode}}$ | $\phi$ | $\Delta I_{\mathrm{estimated}}$ | $\Delta I_{\mathrm{measured}}$ |
|---|---|---|---|---|
| 4.93 V | 1.2 nm | 2.84 eV | 8.4 pA | 7.9 pA |
| 5.15 V | 2 nm | 2.96 eV | 7.2 pA | 7.15 pA |

FIG. 2. (a) Switching between two states of different conductivity (6.0 and 5.7 nm electrical thickness). (b) Two current peaks superposed to the FN current measured on a 3 nm oxide. The table shows the estimated barrier height and the associated current increment when an electron is detrapped from a trap site located 1.2 and 2 nm from the cathode in a 3 nm oxide, when the stress voltage is 4.93 and 5.15 V, respectively. The values obtained are quite close to the magnitude of the current peaks in curve (b).

Sequences of voltage ramps have been applied on fixed oxide locations to measure the effect of the degradation on the electrical properties of the spots (before breakdown takes place). As the number of applied ramps increases (the degradation increases), a shift of the $I-V$ curves to larger/smaller voltages, depending on the oxide thickness, has been observed, i.e., the electrical thickness increases/decreases. On 3 nm thick oxides, $t_{\mathrm{eff}}$ decreases (larger currents are measured for the same voltage); this observation is compatible with trap assisted tunneling through the generated defects.[14] On 6 nm thick oxides, however, larger $t_{\mathrm{eff}}$ are measured, which can be attributed to negative charge trapping in the defects generated.[9] Besides these observations (similar to those in macroscopic tests and also reported in microscopic tests), switching events between two states of well-defined conductivity have also been recorded. As an example, curve (a) [(squares) in Fig. 2] shows a commutation from a state with a small conductivity ($t_{\mathrm{eff}}$=6.0 nm, dashed line) to another with larger conductivity ($t_{\mathrm{eff}}$=5.7 nm, dashed line), which implies a change in current of ~1 pA. Although in this case the two states are quite stable, sudden changes in conductivity [Fig. 2(b)] detected as current peaks superimposed on to the FN characteristics have also been observed. The probability of the occurrence of these events increases with the amount of electrical stress (i.e., the number of voltage ramps previously applied). An analysis of an ensemble of $I-V$ curves shows that the observed peaks are not randomly distributed, i.e., the sudden changes in current are strikingly localized around certain values of the voltage. Additionally, breakdown mostly occurs at those voltages at which the current peaks are most often measured. We suggest that the observed phenomena are related to the degradation induced at the spot, i.e., to the generation of defects and to the trapping/detrapping of individual charges in the generated traps (single electron trapping effects from defects on Si surfaces observed with STM have been already

reported).[15,16] In fact, electrostatic estimations show that the capture/release of an elementary charge (electron or hole) in a trap site leads to changes in current of the same order of magnitude as that of the observed peaks (a few pA). As an example, we have estimated the change in the barrier height and in the current associated to detrapping of an electron from a trap located at different cathode distances, and this can properly explain the current spikes in the 3 nm oxide in Fig. 2 (curve b). The table in Fig. 2 shows that when the detrapping occurs from a trap located at 1.2 (for 4.93 V) and 2 nm (for 5.15 V) the injection barrier height is lowered from 3.15 eV to 2.84 and 2.96 eV, respectively, leading to current increments quite close to the measured values. Since these kinds of events are mainly observed after electrical stress, the trap sites involved must have been generated during the test. All these results point out that the microscopic phenomena observed with the C-AFM may be related to the pre-breakdown noise recently reported in macroscopic tests.[17]

To summarize, a C-AFM has been used to perform stress tests on ultrathin $SiO_2$ to analyze the conduction properties of worn-out oxides at a nanometer scale. In particular, switching between two states of well-defined conductivity and sudden changes in conductivity have been observed before breakdown, and they have been suggested to be related to the pre-breakdown noise measured during macroscopic electrical tests. Therefore, the C-AFM can help to determine the microscopic nature of the degradation process at the same scale at which it takes place.

The authors are grateful to the Dirección General de Investigación Científica y Técnica for partially supporting this work under Project No. BFM2000-0343.

[1] J. Suñé, I. Placencia, N. Barniol, E. Farrés, F. Martín, and X. Aymerich, Thin Solid Films **185**, 347 (1990).
[2] H. Watanabe, K. Fujita, and M. Ichikawa, Appl. Phys. Lett. **72**, 1987 (1998).
[3] E. S. Daniel, J. T. Jones, O. J. Marsh, and T. C. McGill, J. Vac. Sci. Technol. B **15**, 1089 (1997).
[4] H. J. Wen and R. Ludeke, J. Vac. Sci. Technol. A **16**, 1735 (1998).
[5] B. Kaczer and J. P. Pelz, J. Vac. Sci. Technol. B **14**, 2854 (1996).
[6] H. J. Wen and R. Ludeke, J. Vac. Sci. Technol. B **15**, 1080 (1997).
[7] S. J. O'Shea, R. M. Atta, M. P. Murrell, and M. E. Welland, J. Vac. Sci. Technol. B **13**, 1945 (1995).
[8] A. Olbrich, B. Ebersberger, and C. Boit, Appl. Phys. Lett. **73**, 3114 (1998).
[9] A. Olbrich, B. Ebersberger, and C. Boit, 36th Annual IEEE International Reliability Physics Proceedings, Reno, Nevada, 1998, p. 163.
[10] M. Porti, X. Blasco, M. Nafría, X. Aymerich, A. Olbrich, and B. Ebersberger, Microelectron. Reliab. (in press).
[11] A. E. Gordon, R. T. Fayfield, D. D. Litfin, and T. K. Higman, J. Vac. Sci. Technol. B **13**, 2805 (1995).
[12] H. Watanabe, T. Baba, and M. Ichikawa, J. Appl. Phys. **85**, 6704 (1999).
[13] R. H. Fowler and L. Nordheim, Proc. R. Soc. London, Ser. A **119**, 173 (1928).
[14] P. Olivo, T. N. Nguyen, and B. Riccó, IEEE Trans. Electron Devices **20**, 2259 (1988).
[15] M. E. Welland and R. H. Koch, Appl. Phys. Lett. **48**, 724 (1986).
[16] R. H. Koch and R. J. Hamers, Surf. Sci. **181**, 333 (1987).
[17] F. Crupi, B. Neri, and S. Lombardo, IEEE Electron Device Lett. **21**, 319 (2000).